Calcif Tissue Int (2017) 100:87–94
DOI 10.1007/s00223-016-0200-0

ORIGINAL RESEARCH

Unloading-Induced Degradation of the Anisotropic Arrangement of Collagen/Apatite in Rat Femurs

Jun Wang[1] · **Takuya Ishimoto**[2] · **Takayoshi Nakano**[2]

Received: 3 August 2016 / Accepted: 13 October 2016 / Published online: 22 October 2016

Abstract The specific orientation of collagen and biological apatite (BAp) is an anisotropic feature of bone micro-organization; it is an important determinant of bone mechanical function and performance under anisotropic stress. However, it is poorly understood how this microstructure orientation is altered when the mechanical environment changes. We hypothesized that the preferential orientation of collagen/BAp would change in response to changes in mechanical conditions, similar to the manner in which bone mass and bone shape change. In the present study, we investigated the effect of unloading (removal of anisotropic stress) on the preferential orientation of collagen/BAp using a rat sciatic neurectomy model. Bone tissue that formed under unloaded conditions showed a more disordered collagen/BAp orientation than bone tissue that formed under physiological conditions. Coincidentally, osteocytes in unloaded bone displayed spherical morphology and random alignment. To the best of our knowledge, this study is the first to demonstrate the degradation of preferential collagen/BAp orientation in response to unloading conditions. In summary, we identified alterations in bone material anisotropy as an important aspect of the bone's response to unloading, which had previously been examined with regard to bone loss only.

Keywords Unloading · Mechanobiology · Orientation of collagen/apatite · Osteocyte

✉ Takayoshi Nakano
nakano@mat.eng.osaka-u.ac.jp

[1] School of Material Science and Engineering, Zhengzhou University, Zhengzhou 450001, China

[2] Division of Materials and Manufacturing Science, Graduate School of Engineering, Osaka University, 2-1, Yamada-oka, Suita, Osaka 565-0871, Japan

Introduction

Skeletal unloading is a clinically significant condition that results from prolonged bed rest, cast immobilization, musculoskeletal abnormalities (e.g., paralysis and amyotrophy), and arthroplasty-induced stress shielding. Bone tissue has the ability to alter its macroscopic and microscopic architecture to suit its mechanical environment, which is a well-known functional adaptation. A comprehensive understanding of bone responses to unloading or reduced-loading conditions is important for predicting patient bone strength when returning to normal loading conditions.

With regard to bone strength, the preferential orientation of collagen molecules and biological apatite (BAp) nanocrystals significantly contributes to bone material properties. The crystallographic *c*-axes of BAp align with the long axis of collagen fibrils [1] because BAp crystallizes on the collagen template in an epitaxial manner through an in vivo self-assembly process. This anisotropic micro-organization is responsible for the Young's modulus of the bone [2] and the anisotropy in Young's modulus, ultimate stress, and toughness [3]. It is, therefore, important to understand how bone collagen/BAp orientation is altered in response to changes in mechanical conditions.

The adaptive bone response is accomplished by alterations in bone mass or geometry, as assessed by cross-sectional area, second moment of inertia, porosity, bone mineral density (BMD), and other parameters [4–6]. However, the effect of reduced loading on the collagen/BAp orientation is poorly understood, in spite of its relevance to bone strength. We hypothesized that the degree of anisotropy in the preferential collagen/BAp orientation of bones would decrease in response to the removal of the anisotropic stress field, because bone tissue does not require mechanical anisotropy under unloading conditions.

The aim of the present study was to elucidate the responses of bone with respect to material anisotropy. To do so, we assessed the effect of unloading induced by sciatic neurectomy (SN) on the degree of preferential collagen/BAp *c*-axis orientation in rat femurs. In addition, changes in osteocyte morphology were observed because osteocytes are believed to be mechanosensors that may mediate unloading-induced bone responses.

Materials and Methods

Animals and Surgical Operation Procedures

Ten female Sprague–Dawley rats weighing approximately 110 g (aged 4 weeks) were used in this study. All rats were fed commercial food and water ad libitum and were maintained under controlled lighting conditions (12-/12-h light/-dark cycle) throughout the study. The rats were allowed to acclimate for 7 days before the experiment began. They were maintained in normal cage conditions during the acclimation and experiment periods. Following acclimation, five rats were killed as a baseline (BL) group. The other five rats received an SN operation (SN group). Under anesthesia, the sciatic nerves on the lateral side of the proximal femurs were resected by 2–3 mm through a small incision made in the skin. The wound was closed immediately, and the contralateral leg underwent a sham operation and was left intact as a control (CTL group). Sixteen weeks after surgery, the experimental rats were killed. Both the right and left femurs were removed and freed of soft tissues. All femurs were fixed in 70 % ethanol for 48 h and stored in 10 % neutral buffered formalin. Here, the BL group was used to confirm the bone portion that formed under SN-induced unloading condition by comparing bone size and morphology of SN femur with BL ones. All experimental procedures were performed in accordance with the guidelines of the Institutional Animal Care and Use Committee of Daiichi Sankyo Co., Ltd. and the Animal Experiment Committee of the Osaka University Graduate School of Engineering.

Radiography and Femoral Length Measurement

Soft X-ray photographs were taken by using Xie (Chubu Medical, Japan) after femur removal using the following parameters: 40-kV, 40-μA, and 71-ms radiation. Antero-posterior projection was conducted, and femoral length was measured.

Peripheral Quantitative Computed Tomography (pQCT) Analysis for BMD

The volumetric BMD was measured at seven points along the long axis of the femur (points 2–8 in Fig. 1) by pQCT (XCT Research SA+; Stratec Medizintechnik, Germany) with a resolution of 70 μm × 70 μm × 460 μm. A scout view was used to adjust the positions before measurement. A BMD of 690 mg/cm^3 was considered the cortical bone threshold.

Polarized Light Microscopy for Assessing Collagen Orientation

The anterior cortical bone of the femur was decalcified, embedded in paraffin, thinly sectioned along the longitudinal axis, and then deparaffinized. The thin sections were visualized by polarized light microscopy (BX60; Olympus, Japan) with a polarizer and analyzer in cross-position.

Microbeam X-ray Diffraction (μXRD) Analysis for Determining the Degree of Preferential BAp *c*-Axis Orientation

Quantitative crystallographic analysis of the degree of preferential BAp *c*-axis orientation was performed using a μXRD system (R-Axis BQ; Rigaku, Japan) with a transmission optical system, as previously described [7, 8]. The BAp orientation along the long axis of the femur in which the BAp *c*-axis was originally and uniaxially oriented was analyzed [9, 10]. Briefly, Mo-Kα radiation was generated at a tube voltage of 50 kV and a tube current of 90 mA (4.5 kW). The incident beam was focused into a small spot by a double-pinhole metal collimator and radiated vertically to the long axis of the bone. The diffracted X-rays were collected by an imaging plate (IP) placed behind the specimen. The detected diffraction pattern reflected the crystallographic information along the plane vertical to the incident beam that contains the bone long axis. Two peaks from the specific crystallographic plane of BAp (002) and (310) were used to quantitatively analyze the degree of the preferential BAp *c*-axis orientation as the relative ratio of (002) diffracted intensity to (310) intensity. This was previously reported as a suitable index for evaluating BAp orientation [9, 11] and bone mechanical function (Young's modulus) [2]. Randomly oriented hydroxyapatite (NIST #2910: calcium hydroxyapatite) powder had an intensity ratio of 0.8; therefore, values greater than 0.8 indicated the presence of anisotropic BAp *c*-axis orientation in the analyzed direction.

Two types of μXRD measurements were taken. One determined the position dependency of the degree of BAp *c*-axis orientation using the whole bone; the measurements were taken at seven diaphyseal points along the bone's long axis where BMD was measured. An incident beam (300 μm diameter) was radiated in the antero-posterior direction from the anterior surface; therefore, the recorded diffraction reflected the crystallographic information in the

Fig. 1 Soft X-ray photographs of **a** CTL, **b** SN, and **c** BL rat femurs. *Scale bars* 5 mm

anterior and posterior cortices. The measurement duration was 600 s at each point.

The other μXRD measurement was intended to analyze the positional dependency within the cortical bone thickness from the periosteal to endosteal side. After preparing a 500-μm-thick sagittal section from the anterior region using a diamond band saw (BS-300CP; Exakt Apparatebau, Germany), a 100-μm-diameter beam was radiated and the diffraction intensity was collected for 1800 s.

Micro-focused X-ray Computed Tomography (μCT) and Bone Morphological Analysis

Cross-sectional tomographic images were taken utilizing a μCT (SMX-100CT-SV3; Shimadzu, Japan) under 53-kV and 60-μA radiation with a voxel size of 13.45 μm. Following the binarization of μCT images, cross-sectional bone areas and periosteal and endosteal circumferences were measured using Tri/3D-BON (Ratoc System Engineering, Japan) to determine the direction of bone growth upon SN.

Confocal Laser Scanning Microscope Observation of Osteocyte Morphology and Alignment

Anterior cortical bone sections (sagittal plane, ~300 μm thickness) were cut with a diamond band saw and immediately placed in a fixative used for electron microscopy (0.5 % glutaraldehyde and 2 % paraformaldehyde in 0.05 M cacodylate sodium buffer; pH 7.4) [12] for 48 h at room temperature for fixation. Cortical sections were then ground with emery paper (800, 1200 and 2000 grit; Riken, Japan) to a final thickness of approximately 70 μm and dehydrated progressively in 75, 95, and 100 % ethanol for 5 min each.

Osteocytes embedded in the bone matrix were visualized by fluorescent staining [13]. Fluorescein isothiocyanate isomer I (FITC) (F7250; Sigma-Aldrich, USA) diluted to 1 in 100 % ethanol was used to stain lacunae and canaliculi. Specimens were immersed in this solution for 2 h for penetration of the fluorescent dye into the lacunar and canalicular spaces. The cortical specimens were then rinsed in 100 % ethanol, air-dried, and mounted on coverslips with fluorescent mounting medium (Dako North America, USA).

A confocal laser scanning microscope (CLSM) system (FV1000D-IX81; Olympus, Japan) with a UPlanSApo 60× oil objective lens (numerical aperture = 1.35) was used for observation. The frame size of the image was 258 μm × 258 μm (0.5 μm/pixel) with a 16-bit color depth.

Statistical Analysis

The quantitative results were expressed as the mean ± standard deviation (SD). For comparing the CTL and SN

groups, two-tailed paired *t* tests were used. For comparing CTL, SN, and BL groups, one-way analysis of variance (ANOVA) was performed followed by post hoc analysis with a Tukey HSD test. *P* values <0.05 were considered statistically significant. SPSS version 14.0 J software (SPSS Japan Inc., Japan) for Microsoft Windows was used for all statistical analyses.

Results

Effects of SN on Bone Size

All animals remained in good health during the experiment. Figure 1 shows soft X-ray photographs of CTL, SN, and BL femurs. Femoral length did not differ significantly between CTL (35.5 ± 0.4 mm) and SN (35.9 ± 0.2 mm) groups. The SN group femurs showed typical disuse bone atrophy; femoral shaft widths were significantly reduced. Moreover, the marrow space of SN femurs was narrower than that of BL femurs.

BMD and Preferential Orientation of the Collagen/BAp *c*-Axis

As shown in Fig. 2a, BMD varied with position from the proximal to distal regions in both CTL and SN groups, and the maximum BMD values in both groups appeared near the mid-diaphysis. SN did not affect BMD at any region.

The degree of preferential orientation of the BAp *c*-axis [diffracted intensity ratio of (002)/(310)] also showed positional dependence in both CTL and SN groups (Fig. 2b); it peaked at the mid-diaphysis, consistent with the data from a previous report [14]. The intensity ratio along the femur long axis in the proximal diaphysis (points 2–5) of the SN femur was significantly lower than that of the CTL femur.

To identify the bone portion that formed under SN-induced unloading conditions, bone morphology was analyzed at point 4 where the BAp orientation was degraded (Table 1). The cross-sectional bone area of the SN group was significantly higher than that of the BL group, which indicates that bone formation occurred under the unloading conditions. The periosteal circumference length in the SN group was equivalent to that of the BL group, while the endosteal circumference length was significantly lower. This morphometric change indicates that the bone formed predominantly at the endosteal surface under SN.

Figure 3 shows polarized light microscopy images and the distribution of the degree of preferential BAp *c*-axis orientation within the cortical bone thickness at point 4 in the anterior cortex. The homogeneous bright contrast represents homogeneously and preferentially oriented collagen molecules along the bone long axis. The CTL femurs (Fig. 3a) showed more homogeneous collagen alignment along the femur long axis throughout the bone thickness from the periosteum to the endosteum, while disordered collagen directionality was observed in SN femurs, particularly in the endosteal region (Fig. 3b). A corresponding trend is found in the BAp orientation distribution (Fig. 3c), representing a reduction in the degree of BAp orientation along the femur long axis in the endosteal side of cortical bone, which was formed under SN conditions.

Table 1 Bone morphological analysis at point 4 where the preferential orientation was degraded

	Cross-sectional bone area (mm^2)	Periosteal circumferences length (mm)	Endosteal circumferences length (mm)
CTL	6.33 (0.68)[b]	12.03 (0.71)[b]	6.56 (0.81)
SN	3.29 (0.42)[a]	9.11 (0.55)[a]	5.01 (0.66)[a,b]
BL	2.68 (0.08)[a]	9.05 (0.43)[a]	6.32 (0.38)

[a] $P < 0.05$ versus CTL

[b] $P < 0.05$ versus BL

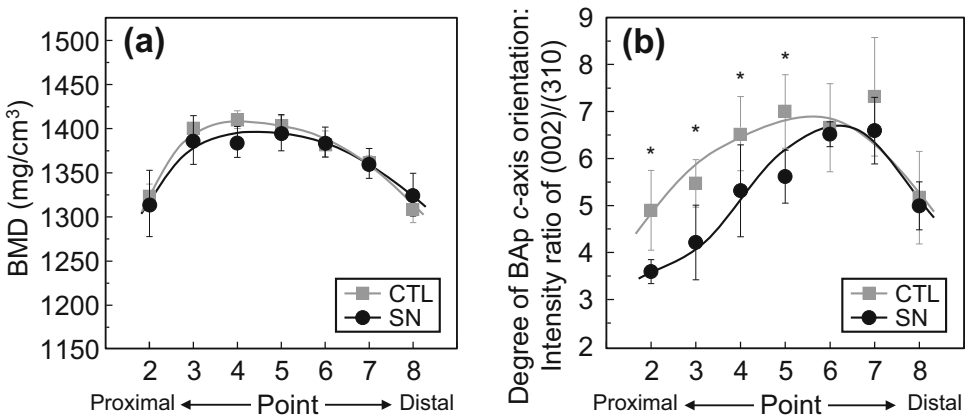

Fig. 2 Distribution of **a** BMD and **b** degree of BAp *c*-axis orientation taken along the femur long axis. *$P < 0.05$ between CTL and SN

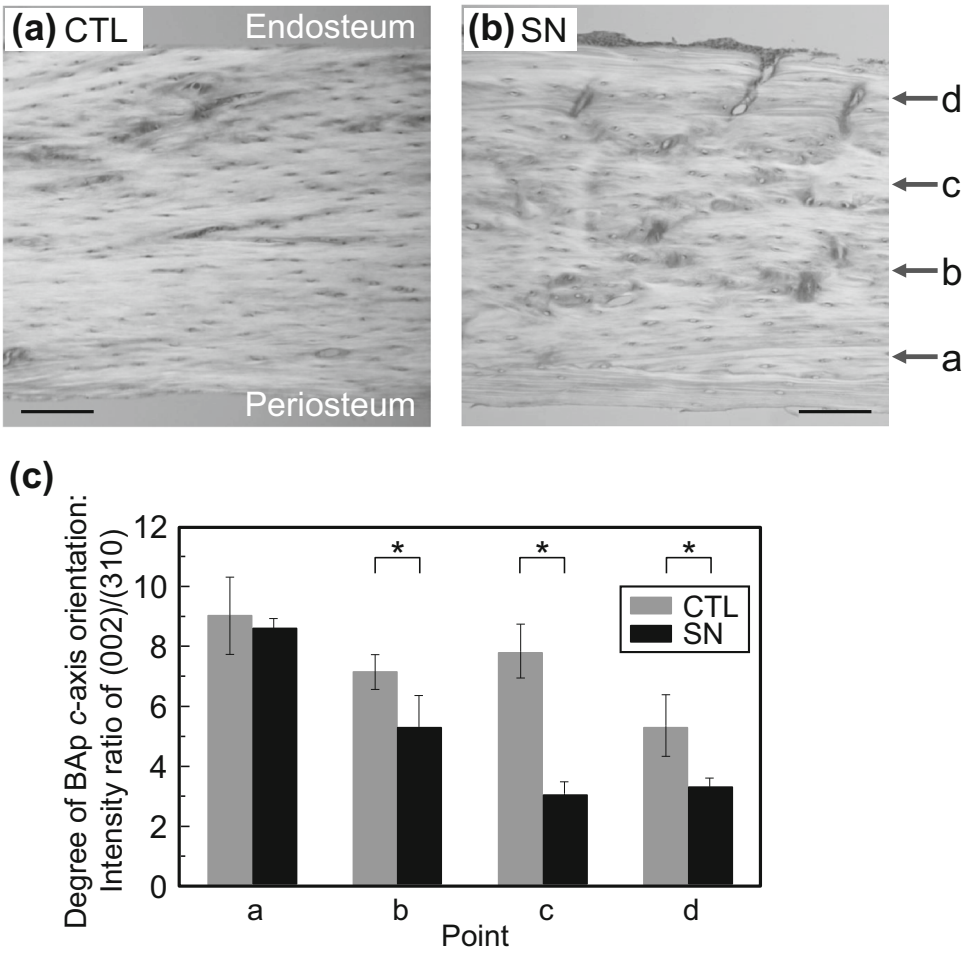

Fig. 3 Polarized light microscopy images of **a** CTL and **b** SN femurs at the anterior cortices of point 4 **c** Distribution of the degree of preferential BAp *c*-axis orientation along the femur's long axis within the bone thickness (periosteal quarter, 1; endosteal quarter, 4) at point 4. *Scale bars* 100 μm. $*P < 0.05$

Osteocyte Morphology and Alignment

Figure 4 shows fluorescently stained lacunae and canaliculi where osteocyte cell bodies and processes reside. The images were taken in the anterior cortices at point 4.

In CTL femurs, osteocytes were elongated and aligned along the long axis of the femur (principal loading direction) throughout the bone thickness (Fig. 4a, b). In contrast, osteocytes at the endosteal side of the cortex in the proximal SN femurs were shaped more spherically and were randomly aligned, which resulted in randomly distributed canaliculi (Fig. 4c, d).

Taken together, both preferential collagen/BAp orientation and osteocyte lacunar and canalicular morphology

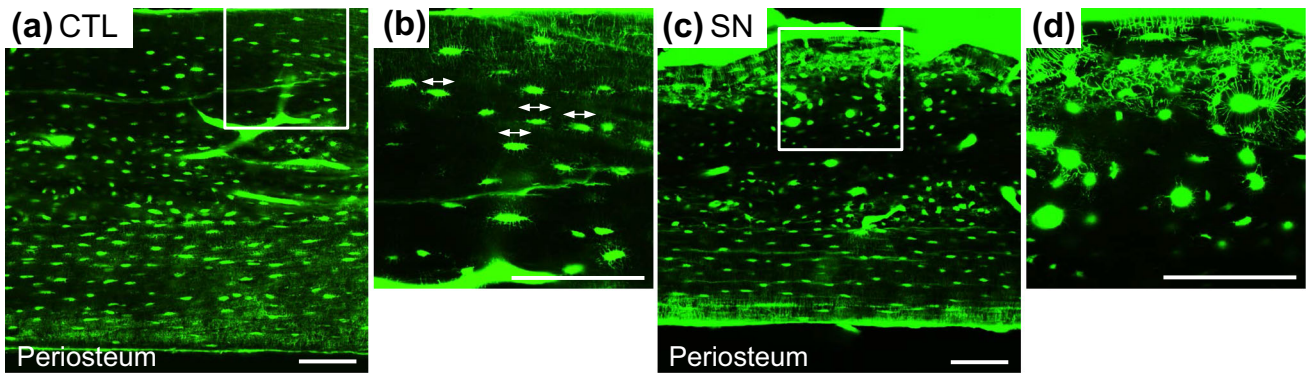

Fig. 4 CLSM images of FITC-labeled osteocyte lacunae and canaliculi around point 4 for **a** CTL and **c** SN femurs, **b**, **d** magnified images of the *boxed regions*. *Scale bars* 100 μm

showed considerable reductions in anisotropy in the endosteal cortex of the SN femurs under unloading conditions.

Discussion

To date, the adaptive responses of bone to its mechanical environment have been considered to include bone formation, bone resorption, and resultant alterations in bone mass [4–6]. Previously, the effects of unloading on bone mass have been investigated using tail suspension [15, 16] and nerve dissection [17, 18] animal models. In humans, studies have investigated the bones of astronauts after space flight [19, 20]. These investigations have revealed significant bone loss under unloading conditions. To our knowledge, no study has investigated the effects of unloading on bone material anisotropy, namely the preferential collagen/BAp orientation, despite the fact that this largely determines bone material properties. To explore this, we used SN as a model of unloading and analyzed the orientation of the collagen/BAp *c*-axis in SN and contralateral CTL femurs. First, we demonstrated the degradation of the anisotropic collagen/BAp *c*-axis orientation upon unloading and the coincident morphological changes in the osteocyte lacunae and canaliculi. This demonstrated the bone's ability to alter its micro-organizational anisotropy in response to changes in external mechanical stimulation.

Consistent with results obtained from previous studies that reported bone loss after SN [17, 21, 22], the present study showed a significant decrease in bone mass in the femoral diaphysis because of SN. This indicated that femurs subjected to SN were immobilized sufficiently to induce bone loss. However, the BMD did not change because of SN, which is similar to the results of a previous study on growing rats [23].

The change in the BAp *c*-axis orientation was position-dependent along the bone's long axis. The proximal diaphysis showed significant degradation in the degree of preferential collagen/BAp orientation, while the distal diaphysis did not show a significant change. A previous study reported that some movements of the upper leg and knee joint persisted even after SN, indicating that the femur was subjected to some position-dependent stress [17]. Therefore, it is possible that the distal femur near the knee joint is subjected to loading even under SN conditions. Another likely reason of the position-dependent change in the BAp *c*-axis orientation is a change in innervation of the limb which was not investigated in this study. Further experiments must be performed to elucidate a direct effect of unloading on the collagen/BAp orientation eliminating the effects of innervation change.

According to our detailed μXRD analysis, the bone tissue that formed under SN condition possessed more isotropic micro-organization than the normally loaded bone, which means that SN caused the reduction in the anisotropy of bone micro-organization in addition to bone loss. From a biomechanics viewpoint, this bone response to unloaded conditions is plausible because bone tissue with more random micro-organization exerts isotropic mechanical properties (e.g., Young's modulus [24]), while oriented collagen/BAp micro-organization results in enhanced mechanical properties in the oriented direction to form mechanical anisotropy [3, 25]. Under unloading conditions, bone tissue does not require mechanical anisotropy. Such unloading-induced alterations in micro-organization are likely to occur under various clinical conditions, including bed rest, cast immobilization, and stress shielding due to metallic implant insertion. It should be noted that these clinical conditions result in more significant declines in mechanical function than would be expected from bone loss alone.

A major challenge for the bone mechanobiology field will be to elucidate the mechanism by which bone tissue responds to its external mechanical environment. Osteocytes are promising candidates for regulating this adaptive bone response. Osteocytes are believed to play an important role in regulating bone mass by recruiting osteoblasts and osteoclasts based on their capability of mechanosensation [26, 27]. Most recently, an important role of osteocytes has been proposed in the regulation of bone microstructure. Shah et al. [28] showed that BAp particles beneath elongated osteocytes tended to align to the osteocyte long axis. Kerschnitzki et al. [29] hypothesized that osteocytes directly control BAp particle orientation, but the details of this process remain undefined.

The present study demonstrated that morphological changes in osteocytes and degradation of the preferential collagen/BAp orientation occurred simultaneously in the same bone region that formed under unloading conditions. The cellular cytoskeleton structure and orientation are reported to be influenced by external mechanical stimuli, especially the direction of principal strain [30, 31], which affects cell shape [30, 32]. Indeed, osteocytes in long bones bearing uniaxial stress have elongated shapes, and they are aligned in the direction of stress [32, 33]. In contrast, osteocytes in less-loaded bones such as the calvaria [32, 33], and unloaded bones [34] have a more spherical shape which are effective in sensing small stimuli [32]. Therefore, it has been hypothesized that osteocytes change their cell shape and cytoskeleton organization to effectively detect the respective mechanical environment [35], thus regulating the formation of the oriented structure according to the mechanical environment they detect.

Using 16-week unloading after SN as a model of unloading, we identified alterations in bone structural parameters and collagen/BAp orientation in rat femurs. However, the effects were different for each parameter measured. According to Frost's mechanostat theory [36], bone mass adapts to stress by different biological processes during four mechanical usage windows, whose thresholds are defined as the minimum effective strains (MESs) for activating the biological process of the adaptive response. The MESs for changes in bone mass have been experimentally demonstrated [6, 37, 38]. We hypothesize that there are MESs for activating adaptive changes in collagen/BAp orientation. It is important to quantitatively define the relationship between collagen/BAp orientation and applied stress, as this will improve our understanding of bone mechanobiology and bone therapy in relation to stress.

In conclusion, the present work first demonstrated the response of bone to SN-induced unloading through degradation of the preferential collagen/BAp *c*-axis orientation. The oriented collagen/BAp micro-organization was highly determined by the applied stress field. Concurrently, osteocyte morphology became more isotropic (spherical) upon SN. Thus, we hypothesized that osteocytes participate in mechanosensation of anisotropic stress fields and regulate the micro-organization of bone tissue. Alterations in the intrinsic material properties of bone in response to changes in the mechanical environment have mechanobiological importance, but this is a poorly studied aspect of bone functional adaptations. In addition to bone mass and bone geometry that have been traditionally considered, future investigations on bone adaptation must consider aspects of bone material anisotropy such as the preferential collagen/BAp *c*-axis orientation.

Acknowledgments This work was partly supported by the Grants-in-Aid for Scientific Research (JP25220912) from the Japan Society for the Promotion of Science (JSPS). The authors thank Chie Fukuda and Shin-ichi Mochizuki of Daiichi Sankyo Co., Ltd. for providing bone specimens.

Author Contributions TN designed the study; JW, TI, and TN conducted the study; JW and TI analyzed the data; TI and TN interpreted the data; JW and TI drafted the manuscript; and all authors revised the manuscript content and approved the final version of the manuscript. TN takes responsibility for the integrity of the data analysis.

Compliance with Ethical Standards

Conflict of interest Jun Wang, Takuya Ishimoto, and Takayoshi Nakano declare that they have no conflict of interest.

Human and Animal Rights and Informed Consent The study was conducted in accordance with the guidelines of the Institutional Animal Care and Use Committee of Daiichi Sankyo Co., Ltd. and the Animal Experiment Committee of the Osaka University Graduate School of Engineering where the studies were conducted.

References

1. Landis WJ (1995) The strength of a calcified tissue depends in part on the molecular structure and organization of its constituent mineral crystals in their organic matrix. Bone 16:533–544
2. Ishimoto T, Nakano T, Umakoshi Y, Yamamoto M, Tabata Y (2013) Degree of biological apatite c-axis orientation rather than bone mineral density controls mechanical function in bone regenerated using recombinant bone morphogenetic protein-2. J Bone Miner Res 28:1170–1179
3. Li S, Demirci E, Silberschmid VV (2013) Variability and anisotropy of mechanical behavior of cortical bone in tension and compression. J Mech Behav Biomed Mater 21:109–120
4. Sample SJ, Collins RJ, Wilson AP, Racette MA, Behan M, Markel MD, Kalscheur VL, Hao Z, Muir P (2010) Systemic effects of ulna loading in male rats during functional adaptation. J Bone Miner Res 25:2016–2028
5. Mosley JR, March BM, Lynch J, Lanyon LE (1997) Strain magnitude related changes in whole bone architecture in growing rats. Bone 20:191–198
6. Sugiyama T, Meakin LB, Browne WJ, Galea GL, Price JS, Lanyon LE (2012) Bones' adaptive response to mechanical loading is essentially linear between the low strains associated with disuse and the high strains associated with the lamellar/woven bone transition. J Bone Miner Res 27:1784–1793
7. Shimomura A, Matsui I, Hamano T, Ishimoto T, Takehana K, Inoue K, Kusunoki Y, Mori D, Nakano C, Obi Y, Fujii N, Takabatake Y, Nakano T, Tsubakihara Y, Isaka Y, Rakugi H (2014) Dietary L-lysine prevents arterial calcification in adenine-induced uremic rats. J Am Soc Nephrol 25:1954–1965
8. Noyama Y, Nakano T, Ishimoto T, Sakai T, Yoshikawa H (2013) Design and optimization of the oriented groove on the hip implant surface to promote bone microstructure integrity. Bone 52:659–667
9. Nakano T, Kaibara K, Tabata Y, Nagata N, Enomoto S, Marukawa E, Umakoshi Y (2002) Unique alignment and texture of biological apatite crystallites in typical calcified tissues analyzed by microbeam X-ray diffractometer system. Bone 31:479–487
10. Sasaki N, Sudoh Y (1997) X-ray pole figure analysis of apatite crystals and collagen molecules in bone. Calcif Tissue Int 60:361–367
11. Nakano T, Kaibara K, Ishimoto T, Tabata Y, Umakoshi Y (2012) Biological apatite (BAp) crystallographic orientation and texture as a new index for assessing the microstructure and function of bone regenerated by tissue engineering. Bone 51:741–747
12. Ciani C, Doty SB, Fritton SP (2009) An effective histological staining process to visualize bone interstitial fluid space using confocal microscopy. Bone 44:1015–1017
13. Kamioka H, Honjo T, Takano-Yamamoto T (2001) A three-dimensional distribution of osteocyte processes revealed by the combination of confocal laser scanning microscopy and differential interference contrast microscopy. Bone 28:145–149
14. Sasaki K, Nakano T, Ferrara JD, Lee JW, Sasaki T (2008) New technique for evaluation of preferential alignment of biological apatite (BAp) crystallites in bone using transmission X-ray diffractometry. Mater Trans 49:2129–2135
15. Basso N, Jia Y, Bellows CG, Heersche JNM (2005) The effect of reloading on bone volume, osteoblast number, and osteoprogenitor characteristics: studies in hind limb unloaded rats. Bone 37:370–378
16. Matsumoto T, Nakayama K, Kodama Y, Fuse H, Nakamura T, Fukumoto S (1998) Effect of mechanical unloading and reloading on periosteal bone formation and gene expression in tail-suspended rapidly growing rats. Bone 22:89S–93S

17. Zeng QQ, Jee WSS, Bigornia AE, King JG Jr, D'Souza SM, Li XJ, Ma YF, Wechter WJ (1996) Time responses of cancellous and cortical bones to sciaticneurectomy in growing female rats. Bone 19:13–21
18. Maïmoun L, Brennan-Speranza TC, Rizzoli R, Ammann P (2012) Effects of ovariectomy on the changes in microarchitecture and material level properties in response to hind leg disuse in female rats. Bone 51:586–591
19. Carpenter RD, LeBlanc AD, Evans H, Sibonga JD, Lang TF (2010) Long-term changes in the density and structure of the human hip and spine after long-duration spaceflight. Acta Astronaut 67:71–81
20. Lang T, LeBlanc A, Evans H, Lu Y, Genant H, Yu A (2004) Cortical and trabecular bone mineral loss from the spine and hip in long-duration spaceflight. J Bone Miner Res 19:1006–1012
21. Yonezu H, Ikata T, Takata S, Shibata A (1999) Effect of sciatic neurectomy on the femur in growing rats: application of peripheral quantitative computed tomography and Fourier transform infrared spectroscopy. J Bone Miner Metab 17:259–265
22. Iwamoto J, Takeda T, Ichimura S, Sato Y, Yeh JK (2003) Comparative effects of orchidectomy and sciatic neurectomy on cortical and cancellous bone in young growing rats. J Bone Miner Metab 21:211–216
23. Yonezu H, Takata S, Shibata A (2004) Effects of unilateral sciatic neurectomy on growing rat femur as assessed by peripheral quantitative computed tomography, Fourier transform infrared spectroscopy and bending test. J Med Invest 51:96–102
24. Ishimoto T, Nakano T, Yamamoto M, Tabata Y (2011) Biomechanical evaluation of regenerated long bone by nanoindentation. J Mater Sci Mater Med 22:969–976
25. Garnero P (2015) The role of collagen organization on the properties of bone. Calcif Tissue Int 97:229–240
26. Burger EH, Klein-Nulend J (1999) Mechanotransduction in bone—role of the lacuno-canalicular network. FASEB J 13(Suppl):S101–S112
27. Klein-Nulend J, van der Plas A, Semeins CM, Ajubi NE, Frangos JA, Nijweide PJ, Burger EH (1995) Sensitivity of osteocytes to biomechanical stress in vitro. FASEB J 9:441–445
28. Shah FA, Zanghellini E, Matic A, Thomsen P, Palmquist A (2016) The orientation of nanoscale apatite platelets in relation to osteoblastic–osteocyte lacunae on trabecular bone surface. Calcif Tissue Int 98:193–205
29. Kerschnitzki M, Kollmannsberger P, Burghammer M, Duda GN, Weinkamer R, Wagermaier W, Fratzl P (2013) Architecture of the osteocyte network correlates with bone material quality. J Bone Miner Res 28:1837–1845
30. Wang N, Butler JP, Ingber DE (1993) Mechanotransduction across the cell-surface and through the cytoskeleton. Science 260:1124–1127
31. Maniotis AJ, Chen CS, Ingber DE (1997) Demonstration of mechanical connections between integrins, cytoskeletal filaments, and nucleoplasm that stabilize nuclear structure. Proc Natl Acad Sci USA 94:849–854
32. Vatsa A, Breuls RG, Semeins CM, Salmon PL, Smit TH, Klein-Nulend J (2008) Osteocyte morphology in fibula and calvaria—is there a role for mechanosensing? Bone 43:452–458
33. Himeno-Ando A, Izumi Y, Yamaguchi A, Iimura T (2012) Structural differences in the osteocyte network between the calvaria and long bone revealed by three-dimensional fluorescence morphometry, possibly reflecting distinct mechano-adaptations and sensitivities. Biochem Biophys Res Commun 417:765–770
34. Sugawara Y, Kamioka H, Ishihara Y, Fujisawa N, Kawanabe N, Yamashiro T (2013) The early mouse 3D osteocyte network in the presence and absence of mechanical loading. Bone 52:189–196
35. Klein-Nulend J, Bakker AD, Bacabac RG, Vasta A, Weinbaum S (2013) Mechanosensation and transduction in osteocytes. Bone 54:182–190
36. Frost HM (2003) Bone's mechanostat: a 2003 update. Anat Rec A 275:1081–1101
37. Turner CH, Forwood MR, Rho JY, Yoshikawa T (1994) Mechanical loading thresholds for lamellar and woven bone formation. J Bone Miner Res 9:87–97
38. Rubin CT, Lanyon LE (1985) Regulation of bone mass by mechanical strain magnitude. Calcif Tissue Int 37:411–417